A correlating receiver for ES-OFDM using multiple antennas

André B.J. Kokkeler and Gerard J.M. Smit
University of Twente
Enschede, The Netherlands
Email: a.b.j.kokkeler@utwente.nl

***Abstract*—Extended Symbol OFDM (ES-OFDM) is applied in case of a multiple antenna receiver. The receiver architecture is based on the observation that OFDM constellation points can be determined by means of correlation. Summing correlations between multiple antennas leads to an interferometer receiver. This approach gives the freedom to choose which correlations are summed. Three antenna structures are explored: a Uniform Linear Array (ULA) and a sparse array where all correlations are summed and a sparse array where only a selection of correlations are summed. The sensitivity of the Bit Error Rate (BER) of an ES-OFDM communication link to an interfering source from different directions is studied.**

The ULA leads to a relatively wide BER main lobe, the range of angles around the Direction of Arrival of the ES-OFDM signal where the BER is high. Outside this range, the interfering source is suppressed to low BERs, in many cases beyond requirements. By using sparse arrays, the width of the BER main lobe can be traded against the BER levels outside the BER main lobe. This effect is shown for a sparse array where all possible correlations are summed. By summing only those correlations that lead to a uniform co-array, BER levels outside the BER main lobe are lower for an interferometer receiver compared to a traditional beamforming receiver.

***Index Terms*—Correlation, Differential phase shift keying, Fourier transforms, Frequency division multiplexing, Modulation, Beamforming, Interferometry, Phased Array**

I. Introduction

Within the telecommunications industry, there is consensus that segmentation of the spectrum has led to inefficient use of both spectrum and energy. In reaction to that, alternatives such as ultra wide band (UWB, [1]) have been introduced with the main characteristic that they operate at very low Signal-to-Noise-Ratio (SNR). Extended Symbol OFDM (ES-OFDM, [2]) is a technique operating at very low SNR. By repetition of OFDM symbols in time at the transmitter, noise is reduced by a cross correlation operation at the receiver. In [3], this is shown for both Additive White Gaussian Noise (AWGN) and Rayleigh fading channels.

Where ES-OFDM exploits the repetition of OFDM symbols in time, multiple antennas can be used to exploit the repetition of symbols in space. In an ES-OFDM receiver, signals from multiple antennas can be combined before or after cross correlation. These techniques are called beamforming and interferometry respectively. Beamforming in communication systems has been studied intensively (see e.g. [4] and [5]). Interferometry has not been given much attention in this context. Therefore, the following research questions are formulated:

- How can an interferometer be used in combination with ES-OFDM?
- Can irregular placement of antennas be exploited?
- Can an interferometer outperform a beamforming receiver?

To answer these questions, we first discuss related work in section II and briefly describe ES-OFDM in section III. Section IV describes how spatial correlation can be exploited. In section V, a general framework is presented for the analysis of ES-OFDM using multiple antennas. This framework is used in three case studies which are described in section VI. The conclusions follow in section VII.

II. Related work

Within radio astronomy, interferometers have been used for decades to produce detailed images of celestial objects [6]. Within telecommunication systems, the use of optical interferometry is widespread [7]. An interferometer to modulate and demodulate carriers in the electronic domain has been used in [8] and related publications. At the receiver, the incoming signal is cross correlated with a set of carriers with known phase offsets. This is fundamentally different from our approach where only signals from receivers, not known a priori, are cross correlated. Besides the above mentioned publications, electronic interferometers have not been researched extensively. This is mainly because their use is only justified in case of a very low or negative SNR, a scenario generally not applicable to contemporary telecommunication systems but which is applicable to ES-OFDM.

Antenna arrays with non regular spacings are also called sparse arrays. Sparse arrays are traditionally used in e.g. radio astronomy [6], Direction of Arrival (DoA) estimation [9] and direction finding through radar [10], but their use in wireless communication systems is limited. In [11], a sparse array is used at the transmitter, where antennas are divided into subarrays creating multiple beams to modulate directional information onto OFDM carriers. The receiver consists of a single antenna. In our approach, a sparse array is used at the receiver to realize a single beam.

III. Extended Symbol OFDM

ES-OFDM has been introduced in [2]. It is based on the repetition of OFDM symbols in time constituting extended

978-1-4673-3122-7/13/$31.00 ©2013 IEEE

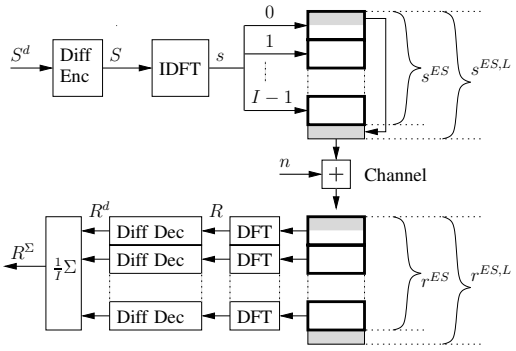

Fig. 1. Base-band equivalent model of differential ES-OFDM

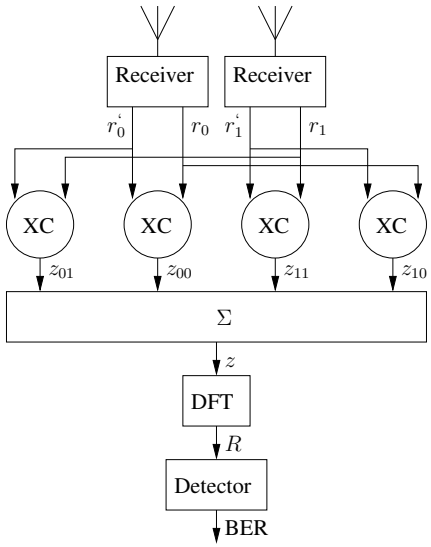

Fig. 2. ES-OFDM inteferometer using two antennas

symbols. To prevent increased sensitivity to local oscilator offsets, data is differentially encoded between adjacent carriers. In this case, cross correlation of two carriers can be used to determine OFDM constellation points. In Fig. 1, we present a base-band equivalent model of a differential ES-OFDM system. At the transmitter, a source produces data vector S^d which consists of $N-1$ complex values where each value is a constellation point from a chosen modulation scheme. S^d is used to modulate carriers S by means of differential encoding S is transformed into the time domain through the IDFT giving s. I copies of s are concatenated giving the extended symbol s^{ES}. The last L samples of s act as a cyclic prefix completing $s^{ES,L}$. The values of this extended symbol are shifted out serially and transmitted through the channel. We assume an additive white Gaussian noise (AWGN) channel adding n to $s^{ES,L}$ resulting in $r^{ES,L}$. In the receiver, the first step is to remove the cyclic prefix, giving r^{ES}. At the receiver, we identify I blocks, where each block contains N samples Each individual block is converted into the frequency domain and differentially decoded. From the I blocks of data, corresponding values are averaged. Neglecting the noise contributions and assuming channel gain equals 1, the output of the receiver equals the transmitter input.

The resulting BER performance after detection in case of BPSK modulated carriers in an Additive White Gaussian Noise (AWGN) channel becomes (see [12] and [2]):

$$\begin{aligned} \mathrm{BER} = & \quad \frac{1}{2^I} e^{-(I\cdot \mathrm{SNR})} \sum_{i=0}^{I} \frac{(I\cdot \mathrm{SNR})^i}{i!} \sum_{j=i}^{I-1} \frac{1}{2^j} C_{j-i}^{j+I-1} \qquad (1) \\ \triangleq & \quad \mathrm{SD}(I, \mathrm{SNR}) \end{aligned}$$

$$C_k^n = \frac{n!}{k!(n-k)!} \qquad (2)$$

where I is the number of times a symbol is repeated and SNR the Signal-to-Noise Ratio at the receiver input. The result is that, as a rule of thumb, the Bit Error Rate (BER) performance at around a BER of 10^{-2}, is improved with approximately 2.1 dB for each doubling of the symbol length.

IV. Exploiting correlation between antennas

Besides copying symbols in time at the transmitter, signals can be replicated in space at the receiver by using multiple antennas and associated frontends. Combining signals can be done before or after correlation. These approaches are called beamforming and interferometry respectively. Our aim is to compare the interferometer with the beamforming receiver. Since beamforming has been researched extensively and is well known, only the interferometer is discussed and illustrated for two receivers in Fig. 2.

Each antenna is attached to a receiver which produces 2 baseband signals, r_a and $r_a^{'}$ ($a = 0, 1$ in case of two antennas) where $r_a^{'} = r_a e^{j\frac{2\pi t}{N}}$. $r_a^{'}$ is a frequency shifted version of r_a where the shift ($\frac{1}{N}$) equals one carrier spacing. For each possible combination of a signal and its frequency shifted counterpart, the signals are correlated (XC) and results are summed. The resulting correlation function z is transformed into the frequency domain by the Discrete Fourier Transform (DFT) after which detection follows.

We use the following definition of crosscorrelation between signals from receivers k and l in case of A receivers

$$z_{kl}(\tau) = \frac{1}{IN} \sum_{t=0}^{IN-1} (r_k(t)^{'})^* \cdot r_l(\mathrm{MOD}(t+\tau, IN)) \qquad (3)$$

where $k = 0, 1, ..., A-1$, $l = 0, 1, ..., A-1$ and MOD indicates the modulus function. By using correlations between receivers, directivity is obtained. Because summation is done after correlation, standard beampatterns cannot be used to determine the directional sensitivity of the array. However, by varying the DoA of an interfering signal and keeping the DoA of the signal of interest fixed, the interference suppression performance of the array can be revealed. Note that the following analysis is valid in case of a single interferer. In case multiple interferers are present, a similar analysis should be performed.

V. General framework

We start the description of the general framework with a few definitions. A linear array is used where the signal of interest s is arriving from incidence angle α and an interfering signal

v from incidence angle β. The signal of interest is an ES-OFDM signal with power σ_s^2, whereas the interfering signal v is an AWGN signal (uncorrelated with s) with power σ_v^2. Receiver noise n is modeled as uncorrelated AWGN with power σ_n^2 for each receiver. The ES-OFDM signal satisfies the narrowband assumption and the array is steered towards this signal by means of phase shifts. For receiver a at position p_a (measured in units of $\frac{1}{2}\lambda$), the critically sampled baseband signal is described by

$$r_a = s + v \cdot e^{j\pi(p_a(\sin\beta - \sin\alpha))} + n_a \cdot e^{-j\pi p_a \sin\alpha} \quad (4)$$

Each receiver also produces the frequency shifted signal r_a‘ where

$$r_a\text{‘} = r_a \cdot e^{j\frac{2\pi t}{N}} = s\text{‘} + v\text{‘} \cdot e^{j\pi(p_a(\sin\beta - \sin\alpha))} + n_a\text{‘} \cdot e^{-j\pi p_a \sin\alpha} \quad (5)$$

where s‘, v‘ and n_a‘ are frequency shifted versions of s, v and n_a respectively. We define a set C of tuples (k, l) where the first element is the receiver index of the non-frequency shifted signal and the second element indicates the receiver index of the frequency shifted signal. The set C defines which crosscorrelations are summed

$$z(\tau) = \frac{1}{|C|} \sum_C z_{kl}(\tau) \quad (6)$$

where $|C|$ indicates the cardinality of set C.

In (1), the relation between the SNR at the input of a single antenna receiver and the resulting BER is given as a function of the extension factor I. To use this expression in case of an interferometer receiver, we first determine SINR_d, the SINR at the detector after correlation and summation, given the powers of the signal, interference and noise at the input of each single receiver. Second, we assume that the signal at the detector is produced by a single correlating receiver. Based on SINR_d (the SINR *after* correlation) SINR_{eq} (the SINR *before* correlation) is determined. This value quantifies the suppression of the noise and interference by the interferometer. We then use the following expression to estimate the BER.

$$\mathrm{BER} = \mathrm{SD}(\mathrm{I}, \mathrm{SINR}_{eq}) \quad (7)$$

In Appendix A, a general expression for SINR_{eq} is determined up to a level where the individual contributions of the signal of interest, the interferer and the receiver noise become visible. In case all possible correlations are summed, the expressions in Appendix A can be simplified as is done in Appendix B, leading to:

$$\mathrm{SINR}_{eq} = \frac{\sigma_s^2}{(\sigma_v^2 |Q_\beta|^2 + \frac{1}{A}\sigma_n^2)} \quad (8)$$

where

$$Q_\beta = \frac{1}{A} \sum_{m=0}^{A-1} e^{j\pi p_m(\sin\beta - \sin\alpha)} \quad (9)$$

To compare the interferometer with a beamformer, we use the general theory presented in [14]. In our case all A antennas are identical and the signals are equally weighted which leads to a so-called aperture function w.

$$\begin{aligned} w(p_k) &= \frac{1}{\sqrt{A}}, \quad k = 0, 1, ..., A-1 \\ &= 0, \qquad \text{otherwise} \end{aligned} \quad (10)$$

The discrete co-array function $c(x)$ is defined as the autocorrelation of the aperture function. The Fourier Transform of the co-array function leads to

$$W_\beta = \frac{1}{A} \sum_{m=0}^{A-1} e^{j\pi p_m(\sin\beta)} \quad (11)$$

where W_β is called the aperture smoothing function, see [14], pg. 92. The underlying assumption there is that the antenna is steered towards broadside which corresponds with $\alpha = 0$ in our situation. Combined with an array gain A (because of the summation of A antenna signals) the SINR after beamforming equals SINR_{eq}, the equivalent SINR in case of an interferometer. This shows that, in case all correlations are summed, the interference suppression performance of an interferometer receiver equals the performance of a beamformer.

VI. Case studies

The performance of an interferometer receiver is compared with the performance of a beamforming receiver through three case studies. In the first case study, a regular array is used. In the second case study, an irregular array is used. In both these case studies, all possible correlations are summed. In the third case study, not all possible correlations are summed in case of an irregular array.

A. Case 1: Regular array, summing all correlations

In this section we analyze the BER performance of an interferometer in case of a regular array where all possible correlations are taken into account. In case of A antennas, $C = \{(k,l) | k \in \{0, 1, ..., A-1\} \wedge l \in \{0, 1, ..., A-1\}\}$ and $p_k = k$ for $k = 0, 1, ..., A-1$. The BER performance is determined using (7) and (8). In Fig. 3, we show the resulting BER performance as a function of the angle of arrival β of the interfering signal in case the signal of interest is received from broadside (α = 0). Five antennas are spaced at $\frac{1}{2}\lambda$ spacing, the SNR ($10\ ^{10}\log\frac{\sigma_s^2}{\sigma_n^2}$) equals -3 dB, the SIR ($10\ ^{10}\log\frac{\sigma_s^2}{\sigma_v^2}$) equals -14 dB and the extension factor I is 64. Relatively low SNR and SIR values, together with a relatively high extension factor have been chosen to clearly illustrate the noise reduction effects of extending symbols and to illustrate the spatial filtering effects of sparse arrays. Results based on (7) and results based on a simulation model are presented. The analytical values and simulations overlap giving a BER pattern with a main beam around 0 radian where the BER is around 0.5. For an absolute angle larger that approximately 0.3 radian, the BER is lower than 10^{-3}.

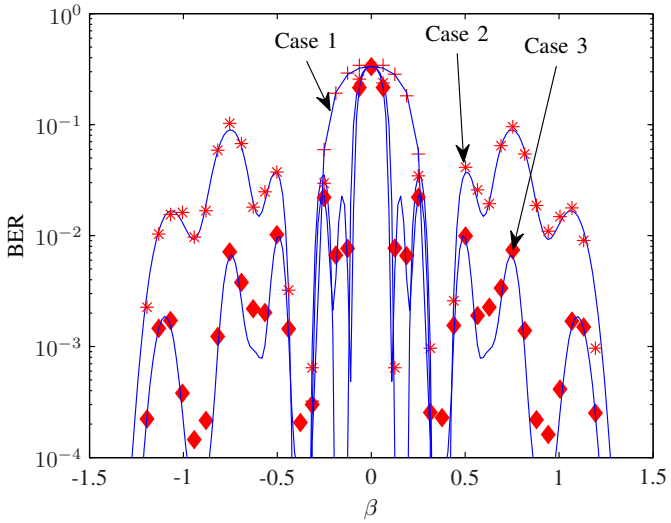

Fig. 3. BER performance in case of a single interferer where all possible correlations are summed and the array is regular (Case 1), the array is irregular (Case 2) and where a selected number of correlations are summed and the array is irregular (Case 3). Markers indicate simulated values, curved lines indicate estimates

B. Case 2: Irregular array, summing all correlations

The BER performance in case of a ULA, as presented in Fig. 3, shows that high BERs are observed at a relatively wide range of angles around the angle of incidence of the desired signal. This range will be refered to as the BER main beam. At the same time the directional sensitivity of the array gives large suppression of the interfering signal at angles relatively far off the angle of incidence of the desired signal. The BER curves at these angles will be refered to as BER sidelobes.

Within communication systems, forward error correcting (FEC) coding and decoding offer bit error correcting capabilities [15], [16]. In [17], it is shown that BERs below 10^{-2} will result in negligible frame error rate probabilities in case of e.g. rate = $\frac{1}{2}$ Viterbi, rate = $\frac{1}{3}$ turbo and rate=$\frac{1}{2}$ MAX-LOG-MAP turbo decoding. Based on this, we assume that before FEC decoding, BERs below 10^{-2} are not required. With respect to the directional BER pattern of Fig. 3, by using sparse arrays, a narrower BER main beam can be traded against higher BER sidelobes without increasing the number of antennas. In a sparse linear array, the distance between adjacent antennas is a multitude of the fundamental spacing. In our case, this is a multitude of $\frac{1}{2}\lambda$ spacing. These arrays are called sparse since not all possible positions within a certain range are actually filled with antennas.

A lot of research has been done on optimal placement of antennas within a sparse array with respect to some beamforming pattern, see e.g. [9]. We will however use the classical Minimum-Redundancy Linear Array as described in [13] to show the effect of irregular antenna spacing and leave the optimization as future work. In [13], for a fixed number of antennas, positions are determined which lead to a co-array with a maximum number of consecutive lags having a non-zero value. For up to 4 antenna elements, antenna spacings can be determined where each possible correlation between antennas corresponds with a unique position within the co-array, except for the correlations of the same receiver. These arrays are called zero-redundancy arrays. In case more than 4 antennas are used, zero-redundancy arrays cannot be constructed but minimum redundancy arrays have been constructed. As an example, we concentrate on the minimum redundancy array which consists of 5 elements as presented in [13]. For this array, the positions are: $p_0 = 0$, $p_1 = 1$, $p_2 = 4$, $p_3 = 7$ and $p_4 = 9$. Thus the aperture function equals

$$\begin{aligned} w(p_k) &= \frac{1}{\sqrt{5}}, \quad k = 0,1,2,3,4 \\ &= 0, \qquad \text{otherwise} \end{aligned} \tag{12}$$

and the discrete co-array:

$$\begin{aligned} c(x) &= \frac{1}{5}, \quad |x| = 1,2,4,5,6,7,8,9 \\ &= \frac{2}{5}, \quad |x| = 3 \\ &= \frac{5}{5}, \quad |x| = 0 \end{aligned} \tag{13}$$

Using the values for p_k mentioned above, Appendix B can be used to determine the BER performance. The BER performance as a function of the angle of arrival β of the interfering signal is presented in Fig. 3, where α = 0. The same settings are used as in Case study 1: SNR = -3 dB, SIR = -14 dB and I = 64 . Both the theoretical results and the results based on the simulation model are presented.

The two expected effects, compared to Case study 1, can be observed; the BER main beam has narrowed while the BER sidelobes are higher.

C. Case 3: Irregular array, summing a selection of correlations

Minimum redundancy arrays still suffer from some redundancy. Even in zero redundancy arrays, the multiple self correlations actually lead to redundancy, see e.g. (13). The general idea behind this third case study is to remove each form of redundancy. Note that this means that a uniform co-array is established. For the 5 element minimum redundancy array, this means that we only use two out of four possible correlations with co-array value $|x| = 3$ and one out of five possible correlations for $|x| = 0$. Note that, instead of summing 25 correlations, we only generate and sum 19 correlations. The required computational capacity is reduced with approximately 24 %. Analysing directivity by means of the co-array is not possible because that approach is based on the assumption that all correlations are used. We therefore start with the analysis in Appendix A. In case of the 5 element minimum redundancy array, the set of tuples C which determines which signals to correlate, is defined as $\{(4,0),(4,1),(3,0),(3,1),(4,2),(2,0),(2,1),(4,3),(1,0),(0,0),(0,1),(3,4),(1,2),(0,2),(2,4),(1,3),(0,3),(1,4),(0,4)\}$. The first element of the lth tuple is indicated as $d_{l,1}$, the second element as $d_{l,2}$. In Appendix C, the different contributions to the SINR for this specific case are determined. The directional sensitivity Q_β of the Signal-Interference and Interference-Noise components and the directional sensitivity P_β of the Interference component are also determined.

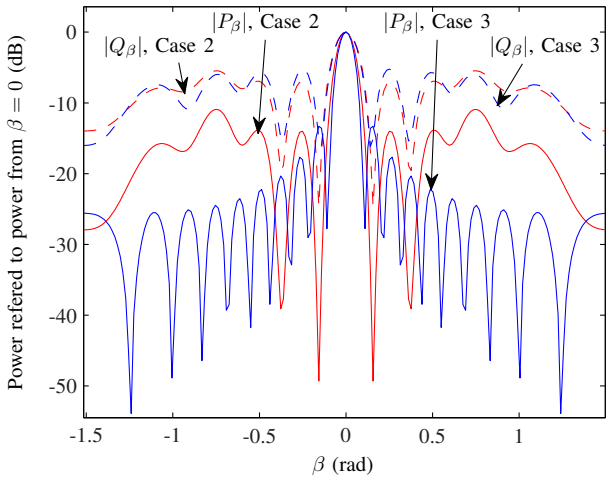

Fig. 4. $|P_\beta|$ and $|Q_\beta|$ in case all possible correlations are summed (Case 2) and in case only a selected number of correlations are summed (Case 3).

In Fig. 4, we show $|Q_\beta|^2$ and $|P_\beta|^2$ for both case studies 2 and 3. For case study 2, $|P_\beta| = |Q_\beta|^2$. For case study 3, $|Q_\beta|$ differs more significantly from $|P_\beta|$. Compared to case 2, the Interference component is suppressed to a larger extent. For $0.5 < |\beta| < 1$, the additional average suppression of the interference component is approximately 10 dB. In Fig. 3, the resulting BER as a function of the incidence angle of the interference is shown.

The main effect is that the error sidelobes are lower enabling acceptable BERs after decoding for a wider range of angles.

VII. Conclusion

In this paper, the use of multiple antennas in a communication system based on ES-OFDM is researched. An interferometer (summation after correlation) and a beamforming receiver (summation before correlation) are compared. Referring to the research questions mentioned in the introduction, it is shown that an interferometer can be used to deliver acceptable BERs when using ES-OFDM. In case all possible correlation functions are summed, the performance of a beamforming receiver and an interferometer are equal.

Irregular arrays give the possibility to reduce susceptibility to interference, resulting in acceptable BERs after coding for a larger range of angles compared to uniform arrays. Performance of the interferometer is further improved, compared to the beamforming receiver, by selecting those correlation functions that establish a uniform co-array. In the specific case studied in this paper, the additional average suppression of an interfering component is approximately 10 dB. In general, being able to select correlation functions is an additional degree of freedom which can be exploited to reduce interference.

References

[1] D. Porcino and W. Hirt, "Ultra-wideband radio technology: potential and challenges ahead," *Communications Magazine, IEEE*, vol. 41, no. 7, pp. 66 – 74, july 2003.

[2] A. B. J. Kokkeler and G. J. M. Smit, "A correlating receiver for ofdm at low snr," in *IEEE 73rd Vehicular Technology Conference Fall (VTC 2011-Spring) , Budapest, Hungary*. USA: IEEE Vehicular Technology Society, May 2011, pp. 1–5.

[3] ——, "Extending ofdm symbols to reduce power consumption," in *Proceedings of the 1st International Conference on Smart Grids and Green IT Systems, Porto, Portugal*. Porto, Portugal: SciTePress, April 2012, pp. 257–262.

[4] J. Litva and T. Lo, *Digital Beamforming in Wireless Communications*. Artech House, 1996.

[5] E. Biglieri, R. Calderbank, A. Constantinides, A. Goldsmith, A. Paulraj, and H. Poor, *MIMO Wireless Communications*. Cambridge University Press, 2007.

[6] A. Thompson, J. Moran, and G. Swenson, *Interferometry and Synthesis in Radio Astronomy*. John Wiley & Sons, 1985.

[7] P. Hariharan, *Optical Interferometry*. Academic Press, 2003.

[8] B. Natarajan, C. Nassar, S. Shattil, M. Michelini, and Z. Wu, "High-performance mc-cdma via carrier interferometry codes," *Vehicular Technology, IEEE Transactions on*, vol. 50, no. 6, pp. 1344 –1353, nov 2001.

[9] Y. I. Abramovich and N. K. Spencer, "Design of nonuniform linear antenna array geometry and signal processing algorithm for doa estimation of gaussian sources," *Digital Signal Processing*, vol. 10, no. 4, pp. 340 – 354, 2000. [Online]. Available: http://www.sciencedirect.com/science/article/pii/S1051200400903786

[10] F. Athley, C. Engdahl, and P. Sunnergren, "On radar detection and direction finding using sparse arrays," *Aerospace and Electronic Systems, IEEE Transactions on*, vol. 43, no. 4, pp. 1319 –1333, october 2007.

[11] T. Hong, M.-Z. Song, and X.-Y. Sun, "Design of a sparse antenna array for communication and direction finding applications based on the chinese remainder theorem," *Progress in Electromagnetics Research*, vol. 98, pp. 119 –136, 2009.

[12] M. Simon and D. Divsalar, "On the implementation and performance of single and double differential detection schemes," *Communications, IEEE Transactions on*, vol. 40, no. 2, pp. 278–291, Feb 1992.

[13] A. Moffet, "Minimum-redundancy linear arrays," *Antennas and Propagation, IEEE Transactions on*, vol. 16, no. 2, pp. 172 – 175, mar 1968.

[14] D. H. Johnson and D. H. Dudgeon, *Array signal processing: Concepts and techniques*. Prentice Hall, 1993.

[15] C. Berrou, A. Glavieux, and P. Thitimajshima, "Near shannon limit error-correcting coding and decoding: Turbo-codes. 1," in *Communications, 1993. ICC 93. Geneva. Technical Program, Conference Record, IEEE International Conference on*, vol. 2, may 1993, pp. 1064 –1070 vol.2.

[16] A. Viterbi, "Error bounds for convolutional codes and an asymptotically optimum decoding algorithm," *Information Theory, IEEE Transactions on*, vol. 13, no. 2, pp. 260 –269, april 1967.

[17] L. T. Smit, G. J. M. Smit, and J. L. Hurink, "Energy efficient wireless communication for mobile multimedia terminals," *Radiomatics - Journal of Communication Engineering special issue on "Advances in Mobile Multimedia"*, vol. 1, no. 1, 2004.

Appendix A

To determine the SINR_d after summation of correlation functions we start with the combination of (3) and (6).

$$z(\tau) = \frac{1}{|C|} \sum_{C} \frac{1}{IN} \sum_{t=0}^{IN-1} (r_k(t)\text{`})^* \cdot r_l(\text{MOD}(t+\tau, IN)) \quad (14)$$

where

$$r_k\text{`} = \quad s\text{`} + v\text{`} \cdot e^{j\pi(p_k(\sin\beta - \sin\alpha))} + n_k\text{`} \cdot e^{-j\pi p_k \sin\alpha} \quad (15)$$

$$r_l = \quad s + v \cdot e^{j\pi(p_l(\sin\beta - \sin\alpha))} + n_l \cdot e^{-j\pi p_l \sin\alpha} \quad (16)$$

Because the noise at the different antennas is mutually uncorrelated, we can skip the exponentials in the last part of (15) and (16). The correlation process results in 9 components. Below, we determine the power of these components separately and lateron use these result to determine the SINR.

- Signal component: $P_{ss} = \sigma_s^4$

- Interference component

$$\begin{aligned} P_{vv} = & \quad \sigma_v^4 \left| \frac{1}{|C|} \sum_C e^{j\pi(p_l(\sin\beta - \sin\alpha) - p_k(\sin\beta - \sin\alpha))} \right|^2 \\ \triangleq & \quad \sigma_v^4 |P_\beta|^2 \end{aligned} \tag{17}$$

- Noise component: $P_{nn} = \frac{1}{|C|}\sigma_n^4$
- The sum of the two Signal-Interference components

$$\begin{aligned} P_{sv} = & \quad \sigma_s^2\sigma_v^2 \left| \frac{1}{|C|} \sum_C e^{j\pi(p_l(\sin\beta - \sin\alpha))} \right|^2 \\ + & \quad \sigma_s^2\sigma_v^2 \left| \frac{1}{|C|} \sum_C e^{-j\pi(p_k(\sin\beta - \sin\alpha))} \right|^2 \\ \triangleq & \quad 2\sigma_s^2\sigma_v^2 |Q_\beta|^2 \end{aligned} \tag{18}$$

- The sum of the two Signal-Noise components

$$\begin{aligned} P_{sn} = & \quad \sigma_s^2 \ \mathrm{E}\left(\left| \frac{1}{|C|} \sum_C n_l \right|^2 \right) \\ + & \quad \sigma_s^2 \ \mathrm{E}\left(\left| \frac{1}{|C|} \sum_C n_k^{'} \right|^2 \right) \end{aligned} \tag{19}$$

  where E indicates the expected value operator.
- The sum of the two Interference-Noise components

$$\begin{aligned} P_{vn} = & \quad \sigma_v^2 \ \mathrm{E}\left(\left| \frac{1}{|C|} \sum_C n_l \cdot e^{-j\pi(p_k(\sin\beta - \sin\alpha))} \right|^2 \right) \\ + & \quad \sigma_v^2 \ \mathrm{E}\left(\left| \frac{1}{|C|} \sum_C n_k^{'} \cdot e^{j\pi(p_l(\sin\beta - \sin\alpha))} \right|^2 \right) \end{aligned} \tag{20}$$

All individual components mentioned above are mutually uncorrelated. We define the power of all crossterms as

$$P_x \triangleq \sigma_x^4 \triangleq P_{sv} + P_{sn} + P_{vn} \tag{21}$$

The general expression for the SINR at the input of the detector (SINR_d) is then given as

$$\mathrm{SINR}_d = \frac{P_{ss}}{P_x + P_{vv} + P_{nn}} \tag{22}$$

where P_{ss} equals the signal power at the input of the detector, P_x the sum of the power of different cross-terms, P_{vv} the power caused by the interference and P_{nn} the noise power generated within the receivers.

Remains to determine the equivalent SINR_{eq} based on SINR_d. In general, in case of a crosscorrelating receiver, an SINR of ρ at the input of a receiver will lead to an SINR of $\frac{\rho^2}{2\cdot\rho+1}$ at the detector. Thus

$$\frac{\mathrm{SINR}_{eq}^2}{2 \cdot \mathrm{SINR}_{eq} + 1} = \mathrm{SINR}_d \tag{23}$$

of which the solution equals

$$\mathrm{SINR}_{eq} = \mathrm{SINR}_d + \sqrt{\mathrm{SINR}_d^2 + \mathrm{SINR}_d} \tag{24}$$

Appendix B

In this appendix, the results from Appendix A are elaborated in case all correlations are summed. The signal component is not affected by the array configuration since it is assumed to be received from broadside. The powers of the remaining components are determined below.

- $P_{vv} = \sigma_v^4 |P_\beta|^2$ where

$$P_\beta = \frac{1}{A^2} \sum_{k=0}^{A-1} \sum_{l=0}^{A-1} e^{j\pi(p_l(\sin\beta - \sin\alpha) - (p_k(\sin\beta - \sin\alpha)))} \tag{25}$$

- $P_{nn} = \frac{\sigma_n^4}{A^2}$
- $P_{sv} = 2\sigma_s^2\sigma_v^2 |Q_\beta|^2$ where

$$Q_\beta = \frac{1}{A} \sum_{m=0}^{A-1} e^{j\pi p_m(\sin\beta - \sin\alpha)} \tag{26}$$

  Note that in this case, $|Q_\beta|^2 = |P_\beta|$.
- $P_{sn} = \frac{2}{A}\sigma_s^2\sigma_n^2$
- $P_{vn} = 2\sigma_v^2 \frac{\sigma_n^2}{A} |Q_\beta|^2$

The power of the so-called crossterms is defined as:

$$P_x = \sigma_x^4 = 2\sigma_s^2\sigma_v^2 |Q_\beta|^2 + 2\frac{\sigma_s^2\sigma_n^2}{A} + 2\frac{\sigma_v^2\sigma_n^2}{A} |Q_\beta|^2 \tag{27}$$

The values given in this appendix can be substituded in (22), resulting in

$$\mathrm{SINR}_d = \frac{\sigma_s^4}{\sigma_x^4 + \sigma_v^4 |P_\beta|^2 + \frac{\sigma_n^4}{A^2}} \tag{28}$$

Using (24) results in

$$\mathrm{SINR}_{eq} = \frac{\sigma_s^2}{(\sigma_v^2 |Q_\beta|^2 + \frac{1}{A}\sigma_n^2)} \tag{29}$$

Appendix C

In this appendix, the values of Q_β, P_β and the power of the Interference-Noise component P_{vn} are determined in the specific case of a sparse array where only a selection of correlations is summed.

$$Q_\beta = \frac{1}{19} \sum_{l=0}^{18} e^{j\pi(p_{d_{l,1}}(\sin\beta - \sin\alpha))} \tag{30}$$

$$P_\beta = \frac{1}{19} \sum_{l=0}^{18} e^{j\pi(p_{d_{l,1}}(\sin\beta - \sin\alpha) - (p_{d_{l,2}}(\sin\beta - \sin\alpha)))} \tag{31}$$

where, $p_0 = 0$, $p_1 = 1$, $p_2 = 4$, $p_3 = 7$ and $p_4 = 9$. Note that in this case, $|P_\beta| \neq |Q_\beta|^2$.

The power of the Interference-Noise component P_{vn} becomes

$$P_{vn} = 2\sigma_v^2 \ \mathrm{E}\left(\left| \frac{1}{19} \sum_{l=0}^{18} n_{d_{l,2}} \cdot e^{j\pi(p_{d_{l,2}}(\sin\beta - \sin\alpha))} \right|^2 \right) \tag{32}$$

Which, in this particular case is approximated by

$$P_{vn} \approx 2\sigma_v^2 \frac{\sigma_n^2}{\sqrt{19}} |Q_\beta|^2 \tag{33}$$

Based on Q_β, P_β and P_{vn}, complemented with the results from Appendix B, (21), (22) and (24) can be used to determine SINR_{eq}.